

# Importance of NKT Cells in Resistance to Herpes Simplex Virus, Fate of Virus-Infected Neurons, and Level of Latency in Mice<sup>∇†</sup>

Branka Grubor-Bauk,<sup>1,2\*</sup> Jane Louise Arthur,<sup>1</sup> and Graham Mayrhofer<sup>2\*</sup>

*Infectious Diseases Laboratories, Institute of Medical and Veterinary Science, Adelaide 5000, Australia,<sup>1</sup> and Discipline of Microbiology and Immunology, School of Molecular and Biomedical Science, University of Adelaide, Adelaide 5005, Australia<sup>2</sup>*

Received 24 January 2008/Accepted 30 June 2008

**Herpes simplex virus type 1 (HSV-1) produces acute mucocutaneous infections, spread to sensory ganglia, and establishment of latency. In addition, neurovirulent strains have potential to invade the central nervous system (CNS), with potentially a lethal outcome. Early activation of defenses at all stages is essential to limit virus load and reduce the risk of neuronal damage, extensive zosteriform skin lesions, and catastrophic spread to the CNS. NKT cells respond rapidly, and we have shown previously that CD1d-deficient mice are compromised in controlling a neuroinvasive isolate of HSV-1. We now compare infection in J $\alpha$ 18 GKO and CD1d GKO mice, allowing direct assessment of the importance of invariant V $\alpha$ 14<sup>+</sup> NKT cells and deduction of the role of the CD1d-restricted NKT cells with diverse T-cell receptors. The results indicate that both subsets of NKT cells contribute to virus control both in the afferent phase of infection and in determining the mortality, neuroinvasion, loss of sensory neurons, size of zosteriform lesions and levels of latency. In particular, both are crucial determinants of clinical outcome, providing protection equivalent to a 1-log dose of virus. These NKT cells can be expected to provide protection at doses of virus that might be encountered naturally.**

The murine zosteriform model of herpes simplex virus type 1 (HSV-1) infection mimics infections that occur in humans (31). During the afferent phase of the infection, the virus replicates in the skin and then enters sensory nerve endings to reach the dorsal root ganglia (DRG), where it undergoes further rounds of replication. This phase is followed by anterograde flow of infectious virus to the skin, giving rise to vesicular bandlike (zosteriform) lesions in the dermatomes supplied by the infected ganglia. In severe infections, the virus may also spread to adjacent DRG and to the central nervous system (CNS). Adaptive immunity is vital for limiting virus replication in the DRG, anterograde spread to the respective dermatomes, and extension to the CNS (for a review, see reference 21). HSV-1 spread to the DRG gives rise to life-long latent infection of sensory neurons, thought to be kept in check by adaptive immunity (for a review, see reference 20).

The precise mechanisms that determine the outcome of HSV-1 infection are complex and incompletely understood (21, 28). Innate immune mechanisms, including interferons and NK cells, limit the local spread of the virus and its entry into sensory nerve endings at sites of infection (37). As adaptive immunity develops, T cells become dominant factors in determining outcome. Although the antiviral actions of CD4<sup>+</sup> T cells are confined mainly to the formation and severity of zosteriform lesions in the skin (24), virus-specific CD8<sup>+</sup> T cells

are important in reducing the severity of zosteriform lesions (43), in protecting infected neurons in DRG from destruction, and in clearing infectious virus (32). These T cells are also thought to play a major part in the long-term containment of latent infection within the DRG (23).

We have shown recently that CD1d-dependent NKT cells are important in the early stages of the immune response to HSV-1 (15). Others have made similar observations in infections with other viruses (13, 18, 40). NKT cells are a unique subset of T cells that express the  $\alpha\beta$  T-cell receptor (TCR) and markers associated usually with NK cells (for reviews, see references 22 and 38). They are comprised mainly of CD4<sup>+</sup> or double-negative cells that express relatively invariant rearrangements of the TCR- $\alpha$  chain (type I NKT cells), as well as others that utilize more diverse rearrangements of genes encoding the TCR (type II NKT cells). The TCR of invariant NKT cells is encoded by gene rearrangements that include the V $\alpha$ 14-J $\alpha$ 18 and V $\beta$ 8, V $\beta$ 7.2, or V $\beta$ 2 gene segments in mice and the homologous V $\alpha$ 24-J $\alpha$ 18 and V $\beta$ 11 gene segments in humans. NKT cells recognize self and exogenous glycolipids presented by antigen-presenting cells in the context of CD1d (for a review, see reference 41). In the case of type I NKT cells, selective stimulation with the CD1d restricted glycolipid  $\alpha$ -galactosylceramide ( $\alpha$ -GalCer) (5, 19) leads to rapid production of both gamma interferon (IFN- $\gamma$ ) and interleukin-4 (IL-4) (5, 19). The downstream effects of NKT cell activation on dendritic cells, B cells, T cells, and NK cells are thought to play an important role in regulating and polarizing immune responses and by acting as a link between innate and adaptive immunity (7, 29, 38).

Because the two subsets of NKT cells have functional differences (22), we compared the responses to infection with a neuropathic strain of HSV-1 (SC16) in mice that either lack all NKT cells (CD1d GKO mice) or are deficient in invariant V $\alpha$ 14<sup>+</sup> NKT cells (J $\alpha$ 18 GKO mice). The results show that

\* Corresponding author. Mailing address for B. Grubor-Bauk: TGR BioSciences Pty Ltd., 31 Dalglish St., Thebarton 5031, Australia. Phone: (61) 8 83546145. Fax: (61) 8 83546188. E-mail: brankagb@tgr-biosciences.com.au. Mailing address for G. Mayrhofer: School of Molecular and Biomedical Science, University of Adelaide, Adelaide 5005, Australia. Phone: (61) 8 83034632. Fax: (61) 8 83034362. E-mail: graham.mayrhofer@adelaide.edu.au.

† Supplemental material for this article may be found at <http://jvi.asm.org/>.

<sup>∇</sup> Published ahead of print on 9 July 2008.

lack of NKT cells has detrimental effects on the containment of the infection to the peripheral nervous system, the fate of infected neurons in DRG, and the establishment of latency. Importantly, the pattern of disease and the level of resistance to fatal infection both depend critically on the dose of virus. Our studies indicate that at doses of a virulent clinical isolate of HSV-1 that produce subclinical or mild infections in normal mice, infections are either severe or lethal in mice that are deficient in NKT cells.

#### MATERIALS AND METHODS

**Virus.** The study used a well-characterized oral isolate of HSV type 1, strain SC16 (17), which has low number of passages in Vero cells and is neuroinvasive in mice. The virus was grown and titrated in Vero cells and a cell-free virus suspension was produced by removal of cells and cell debris by low-speed centrifugation. Cell-free virus was stored at  $-70^{\circ}\text{C}$ .

**Mice.** Specific pathogen-free (SPF) C57BL/6 mice were obtained from the animal facility at the University of Adelaide and kept in SPF conditions in the animal house of the Institute of Medical and Veterinary Science. Breeding pairs of GKO mice (backcrossed from 129 to C57BL/6 background 10 to 12 times) were a generous gift from Mark Smyth, Peter MacCallum Cancer Institute, Melbourne, Australia. These B6.CD1d-deficient (27) and B6.J $\alpha$ 18 deficient (9) mice were bred under SPF conditions at the animal house of the Institute of Medical and Veterinary Science and maintained in SPF conditions during experimentation. All experiments were performed with 6- to 8-week-old mice under approval by the Animal Ethics Committee of the Institute of Medical and Veterinary Science.

**Zosteriform model of infection.** The zosteriform model of infection is as described previously (31). Briefly, the left flank of each mouse was clipped and depilated with Nair cream (Carter-Wallace, Australia), and a 20- $\mu\text{l}$  droplet containing  $10^6$  PFU of virus (unless otherwise indicated) was applied to the flank, dorsal to the posterior tip of the spleen, and corresponding to the tenth thoracic dermatome. Using a 27G needle, the skin was scarified 20 times through the droplet of virus suspension. The virus suspension was removed by blotting approximately 30 s after completion of scarification. Infected mice develop a primary vesicular lesion at the inoculation site, and a characteristic bandlike zosteriform lesion appears 5 to 6 days after virus inoculation, indicating the spread of virus in the peripheral nervous system. The width of the zosteriform lesion (in millimeters) was used as a measure of severity of skin infection and spread to additional DRG and dermatomes. In each experiment, an aliquot of the inoculum was assayed to verify the accuracy of the infectious dose.

**Isolation of replicating virus and measurement of virus titer.** At various times after infection, mice were killed to remove a 1-cm<sup>2</sup> piece of skin that encompassed the inoculation site. The left thoracic DRG were also removed, including those that spanned the 8th through the 13th thoracic segments. The ganglia from each experimental animal were pooled for analysis of infectious virus content. All tissues samples were placed in Dulbecco modified Eagle medium and frozen at  $-70^{\circ}\text{C}$  until required. The presence of infectious virus was determined by homogenizing the tissues and testing 10-fold dilutions of the homogenates on cultures of Vero cells (30).

**Immunohistochemical detection of HSV antigens.** DRG were fixed at room temperature for 1 h in freshly prepared paraformaldehyde-lysine-periodate fixative (26) and embedded in paraffin. HSV antigens were detected in 5- $\mu\text{m}$  sections of ganglia, using the indirect peroxidase-antiperoxidase method, as described previously (33). Briefly, bound rabbit anti-HSV antibody was detected using swine anti-rabbit immunoglobulin, followed by a rabbit peroxidase-antiperoxidase conjugate (Dako, Denmark). Nonspecific binding sites were blocked with 10% normal swine serum in Tris-buffered saline, prior to the addition of primary antibody, and all antibodies were prepared in this diluent. Negative control slides, incubated with diluent instead of primary antibody, were included in each staining run. Slides stained for immunohistochemistry were counterstained with hematoxylin, while others used for routine morphological examination were stained with hematoxylin and eosin. For morphological examination, ganglia from each mouse were embedded in a single block and from a minimum of 70 sections per block; approximately 20 were selected at random for examination. Thus,  $\sim$ 400 sections, from a total of  $\sim$ 1,400, were examined for each mouse strain.

**Detection of latent virus in DRG by nonisotopic in situ hybridization.** Ganglia (T8 to T13) ipsilateral and contralateral to the site of infection were removed 30 days postinfection (p.i.) from five surviving mice from each group, fixed in

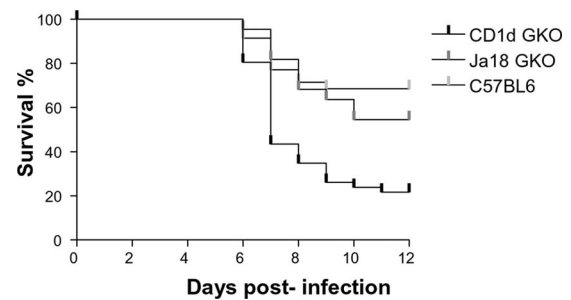


FIG. 1. Survival of NKT-cell-deficient mice infected with neurovirulent HSV-1 (SC16). Groups of CD1d GKO, J $\alpha$ 18 GKO, and C57BL/6 mice ( $n \sim 30$  for each strain) were infected as described in Materials and Methods with  $10^6$  PFU of virus and monitored daily for clinical signs of disease. Mice that were unable to walk and access food/water due to hind limb paralysis were euthanized and are included in the total mortality. The data were analyzed by using the Kaplan-Meier method: CD1d GKO versus J $\alpha$ 18 GKO,  $P = 0.0001$ ; CD1d versus C57BL/6,  $P = 0.0001$ ; and J $\alpha$ 18 GKO versus C57BL/6,  $P = 0.01$ .

periodate-lysine-paraformaldehyde, and embedded in paraffin. From a minimum of 70 sections cut, at least 20 were selected randomly for in situ hybridization to detect latency-associated transcript (LAT) RNA. For detection of the major LATs by in situ hybridization, digoxigenin (DIG)-labeled RNA probes complementary to HSV strain 17 nucleotides 119292 to 120078 were generated and used as previously described (2). Hybridizations were carried out overnight at  $65^{\circ}\text{C}$  ( $25^{\circ}\text{C}$  below the theoretical melting temperature,  $T_m = 90^{\circ}\text{C}$ ), and unbound probe was removed by washing in  $0.1\times$  SSC ( $1\times$  SSC is 0.15 M NaCl plus 0.015 M sodium citrate)–30% deionized formamide–10 mM Tris-HCl (pH 7.5) at  $15^{\circ}\text{C}$  below the  $T_m$  ( $75^{\circ}\text{C}$ ). Bound probe was detected with alkaline phosphatase-conjugated Fab anti-DIG fragments according to the manufacturer's instructions (Roche, Germany). Slides were washed in water and counterstained with rapid hematoxylin for 30 s.

**Enumeration of LAT<sup>+</sup> ganglia and LAT<sup>+</sup> neurons.** To enumerate LAT<sup>+</sup> cells in DRG, a minimum of 70 sections were cut from each block (containing the ganglia collected from five mice) and, from these,  $\sim$ 20 were selected at random for staining. After in situ hybridization, counts were made of the total number of ganglia per section, the number LAT-containing ganglia (LAT<sup>+</sup>) per section and of the total number of LAT<sup>+</sup> neurons within individual LAT<sup>+</sup> ganglia. The percentage of LAT<sup>+</sup> ganglia was obtained for each ganglionic profile by dividing the number of LAT<sup>+</sup> ganglia by the total number of ganglia observed. LAT<sup>+</sup> neurons within the cross-sections of individual ganglia were counted to give an estimate of the number of LAT<sup>+</sup> neurons per ganglionic profile. This method of enumeration has an accuracy of  $\pm 5\%$  (35).

**Statistics.** Virus titers were expressed as  $\log_{10}$  PFU (geometric mean  $\pm$  the standard deviation [SD]), while the sizes and width of zosteriform lesions were recorded in millimeters. Significance was determined by using either a two-tailed unpaired  $t$  test (for comparison of two groups of mice) or by one-way analysis of variance (ANOVA) with Tukey's post hoc test (for comparison of three groups of mice). Survival was analyzed by using the Kaplan-Meier test.

#### RESULTS

**Role of V $\alpha$ 14<sup>+</sup> NKT cells in preventing lethal HSV-1 infection and reducing the severity of skin lesions.** Our previous study (15) showed that virus load and clearance of HSV-1 (SC16) from DRG was approximately equivalent in CD1d GKO mice and in J $\alpha$ 18 GKO mice. We now examine the significance of V $\alpha$ 14<sup>+</sup> NKT cells in determining the outcome of infection by comparing wild-type (wt) mice (NKT cell replete), J $\alpha$ 18 GKO mice (lacking only invariant V $\alpha$ 14<sup>+</sup> NKT cells [21]), and CD1d GKO mice (lacking all NKT cells). As shown in Fig. 1, survival over the 30 days of observation after infection with  $10^6$  PFU (our standard dose) of HSV-1 strain SC16 was 70% in wt mice (26/35), 54% in J $\alpha$ 18 GKO mice

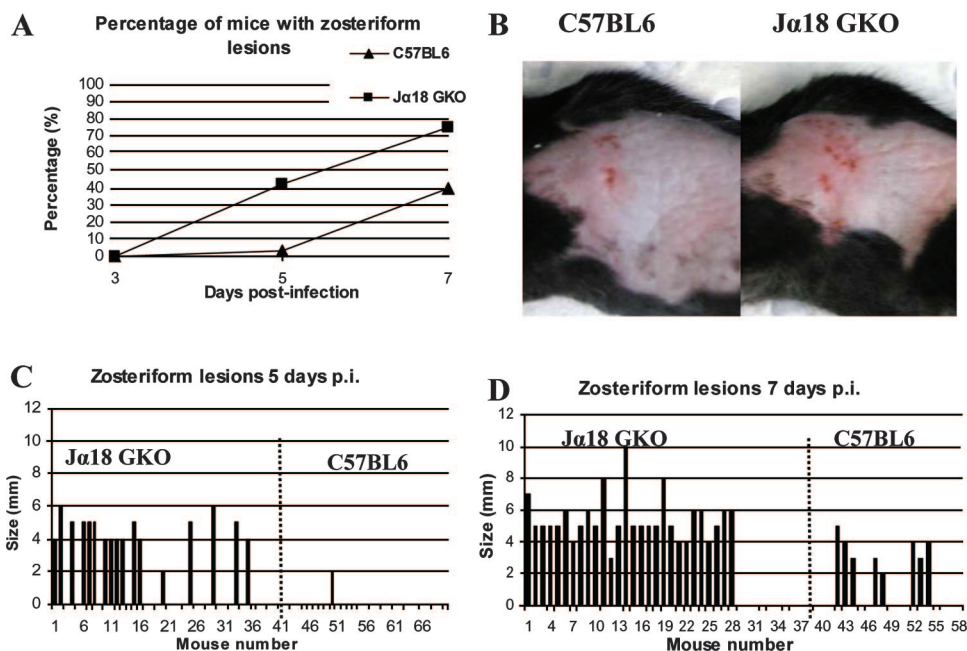


FIG. 2. Progression of zosteriform disease in J $\alpha$ 18 GKO mice. J $\alpha$ 18 GKO ( $n = 41$ ) and C57BL/6 mice ( $n = 28$ ) were infected with  $10^6$  PFU of HSV-1 (SC16) and the incidence and severity of zosteriform lesions examined at days 3, 5, and 7 p.i. (A) Zosteriform lesions appeared earlier in J $\alpha$ 18 GKO mice, and the incidence was higher than in C57BL/6 mice. (B) At 5 days after infection, lesions in J $\alpha$ 18 GKO mice were more extensive than in controls. (C) Widths of zosteriform lesions in individual J $\alpha$ 18 GKO mice (numbers 1 to 41) and C57BL/6 mice (numbers 41 to 69) at day 5 after infection. The lesions of J $\alpha$ 18 GKO mice were significantly larger than those of C57BL/6 mice ( $P = 0.0002$ ). (D) Widths of lesions in remaining J $\alpha$ 18 GKO mice (numbers 1 to 38) and C57BL/6 mice (numbers 38 to 58) at day 7 after infection. The lesions of J $\alpha$ 18 GKO mice were significantly larger than those of C57BL/6 mice ( $P = 0.0003$ ). Significance was determined by using a two-tailed unpaired  $t$  test.

(18/33), and only 33% in CD1d GKO mice (15/46). Notably, there was a significant difference in survival between CD1d GKO and J $\alpha$ 18 GKO mice ( $P = 0.0001$ ) as determined by the Kaplan-Meier method.

Comparison of J $\alpha$ 18 GKO mice and C57BL/6 mice infected with the standard dose of HSV-1 (SC16) showed that V $\alpha$ 14<sup>+</sup> NKT cells also affect the development of zosteriform lesions. By day 5 p.i., 42% (17/41) of the J $\alpha$ 18 GKO mice had developed lesions compared to only ~2% (1/35) of the wt mice (Fig. 2A), and these proportions increased to 74% (28/38) and 40% (8/20), respectively, by day 7 p.i. Throughout the course of the infection, lesions in J $\alpha$ 18 GKO mice were more severe than those observed in controls (Fig. 2B). Shown numerically (Fig. 2C), only one wt mouse had a small zosteriform lesion (~2 mm in width) at day 5 p.i., whereas 17 (42%) of the J $\alpha$ 18 GKO mice developed lesions by this time (mean width of 4.5 mm). By day 7 p.i. (Fig. 2D), 74% of J $\alpha$ 18 GKO mice had zosteriform lesions (mean width of 5 mm), compared to only 40% of wt mice (mean width of 3.5 mm). The differences in size of zosteriform lesions between wt and J $\alpha$ 18 GKO mice were significant at both day 5 ( $P = 0.0002$ ) and day 7 ( $P = 0.0003$ ). We conclude that the lack of V $\alpha$ 14<sup>+</sup> NKT cells allows greater virus replication and spread in J $\alpha$ 18 GKO mice than in wt mice, leading to increased mortality and more extensive lesions in the affected dermatomes. Nevertheless, J $\alpha$ 18 GKO mice appear to be advantaged in terms of survival compared to CD1d GKO mice, indicating an effect of NKT cells with variable TCRs on the final outcome of HSV-1 infection.

**Lack of V $\alpha$ 14<sup>+</sup> NKT cells allows greater virus replication and prolonged viral antigen expression in the DRG.** During HSV-1 infection in wt mice, replication in the DRG is followed by reemergence of infectious virus in the skin by day 5 p.i. High levels of infectious virus can be recovered from the zosteriform lesions at this time. By day 7 p.i., however, most of the virus has been cleared from both the DRG and the skin and healing has commenced (34).

To examine whether control of virus replication in the skin involves V $\alpha$ 14<sup>+</sup> NKT cells, wt and J $\alpha$ 18 GKO mice were infected with the standard dose of HSV-1 (SC16). On days 3, 5, and 7 after inoculation, mice were killed, and a 10-mm square of skin encompassing the inoculation site was excised from each to assay infectious virus. The virus titer ( $\log_{10}$  PFU, means  $\pm$  the SD) in skin (Fig. 3A) was ~100-fold higher ( $6.8 \pm 0.21$ ,  $n = 10$ ) in of J $\alpha$ 18 GKO mice than in wt mice ( $4.7 \pm 0.5$ ,  $n = 10$ ) at day 3 p.i. The differences diminished but remained ~5-fold at day 5 ( $6.88 \pm 0.57$  and  $6.46 \pm 0.32$ , respectively,  $n = 10$ ) and ~10-fold at day 7 ( $5.5 \pm 0.32$  and  $4.6 \pm 0.42$ , respectively,  $n = 5$ ). Differences in virus titers between wt and J $\alpha$ 18 GKO mice were significant at day 3 ( $P < 0.0001$ ) and day 7 ( $P = 0.02$ ).

The virus titer was examined also in the pooled DRG from each mouse (Fig. 3B). Throughout the course of the infection, virus titer in the DRG pooled from individual J $\alpha$ 18 GKO mice was ~10-fold higher than observed in the corresponding ganglia from wt mice. These differences were significant at each time point ( $P < 0.0001$ ), and the respective titers ( $\log_{10}$  PFU, means  $\pm$  the SD) were  $3.8 \pm 0.4$  and  $2.6 \pm 0.39$  on day 3 p.i.

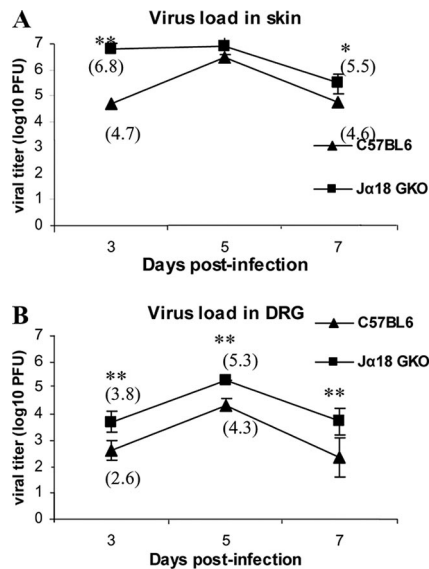


FIG. 3. Kinetics of viral replication in skin and DRG from Jα18 GKO mice. Groups of Jα18 GKO and C57BL/6 mice ( $n = \sim 30$ ) were infected with  $10^6$  PFU of HSV-1 (SC16), and the titers of infectious virus were estimated in skin and DRG of surviving mice at the times shown. Virus titers are expressed as the  $\log_{10}$  PFU (geometric mean  $\pm$  the SD) in homogenates prepared from 10-mm<sup>2</sup> pieces of skin from the zosteriform lesions (A) and from the pooled ipsilateral DRG (B) from each mouse. Significance was determined by using a two-tailed unpaired *t* test; asterisks indicate the days where Jα18 GKO mice had significantly higher virus titers than C57BL/6 mice (\*,  $P = 0.02$ ; \*\*,  $P < 0.0001$ ).

( $n = 10$ );  $5.3 \pm 0.32$  and  $4.3 \pm 0.25$  on day 5 p.i. ( $n = 10$ ) and  $3.73 \pm 0.5$ ,  $2.33 \pm 0.75$  on day 7 p.i. ( $n = 5$ ).

DRG for immunohistochemical studies were obtained from groups of Jα18 GKO and wt mice after infection with the standard dose of HSV-1 (SC16). In DRG prepared from wt mice, virus antigen-positive neurons were rare by day 7 p.i. (Fig. 4B and C). In contrast, most of the DRG from Jα18 GKO mice contained many antigen-positive neurons (Fig. 4A). It appears, therefore, that clearance of HSV from DRG in mice is delayed in mice that lack  $V\alpha 14^+$  NKT cells and that more neurons are infected, either directly via anterograde spread from the skin or by interneuronal spread. Taken together, the findings in skin and DRG indicate that  $V\alpha 14^+$  NKT cells contribute to the control of primary HSV-1 infection by reducing acute viral replication in the skin, reducing viral loads in the DRG, and possibly by reducing interneuronal spread.

**Fate of HSV-1-infected neurons in CD1d GKO and Jα18 GKO mice.** DRG were obtained from CD1d GKO, Jα18 GKO, and wt mice ( $n = 20$  per strain) 6 days after infection with a standard dose of HSV-1 (SC16) and processed for histology. The cell bodies of primary sensory neurons are identified readily by their large size and characteristic appearance (Fig. 5A and B). Although a mononuclear inflammatory infiltrate surrounded many neurons in acutely infected ganglia from wt mice (Fig. 5B), the neuronal architecture was well preserved. The neurons showed no obvious nuclear changes or shrinkage from surrounding support cells (Fig. 4B). In contrast, the neuron bodies in DRG from CD1d GKO mice were vacuolated, and many had retracted from the supporting satellite

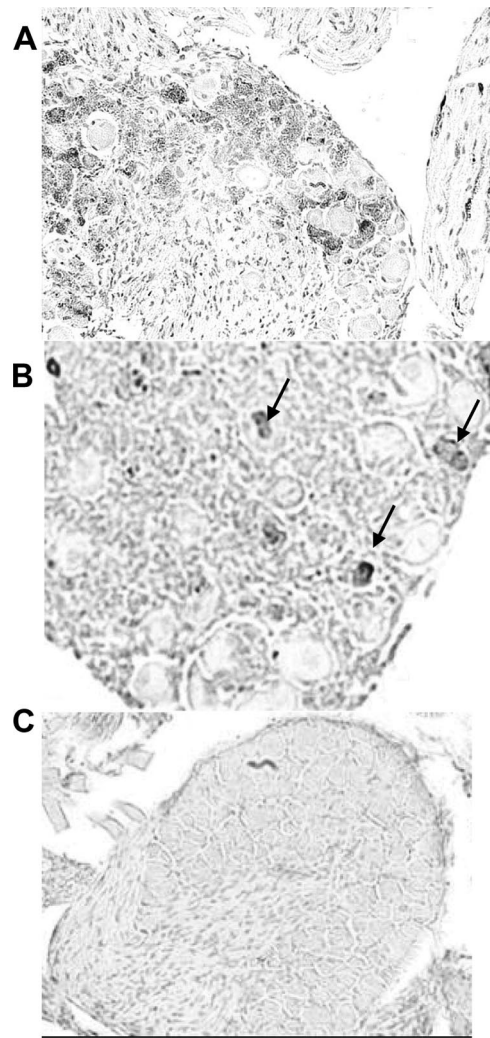


FIG. 4. Sections of DRG obtained from mice at 7 days p.i. with  $10^6$  PFU of HSV-1 (SC16). (A) A ganglion from a Jα18 GKO mouse contains many HSV-1 antigen-positive (dark staining) neurons. Ganglia from wt C57BL/6 mice show profiles of three (arrowed) virus antigen-positive neurons (B) or the absence of virus antigen (C). A and B,  $\times 20$  objective; C,  $\times 10$  objective.

cells (Fig. 5D). Extensive spaces between neurons in the sensory ganglia from these mice, and spaces surrounded by satellite cells, indicated that many neurons had been destroyed (Fig. 5C). In DRG from Jα18 GKO mice, there was also vacuolation of the neuron cytoplasm, shrinkage from the supporting satellite cells (Fig. 5E and F) and reduction in frequency of neurons (Fig. 5E). Overall, the loss of neurons did not appear as marked as in CD1d GKO mice (data not shown). The neuronal changes and loss of neurons in ganglia from Jα18 mice suggest that  $V\alpha 14^+$  (type I) NKT cells play an important role in protection of neurons during acute HSV-1 infection. Nevertheless, the greater damage in DRG from CD1d GKO mice suggests that type II NKT cells also contribute to defense in the peripheral nervous system.

**Differences in outcomes of infection in CD1d GKO, Jα18GKO, and wt mice, revealed by inoculation with lower doses of HSV-1.** Whereas the viral loads in the individual DRG

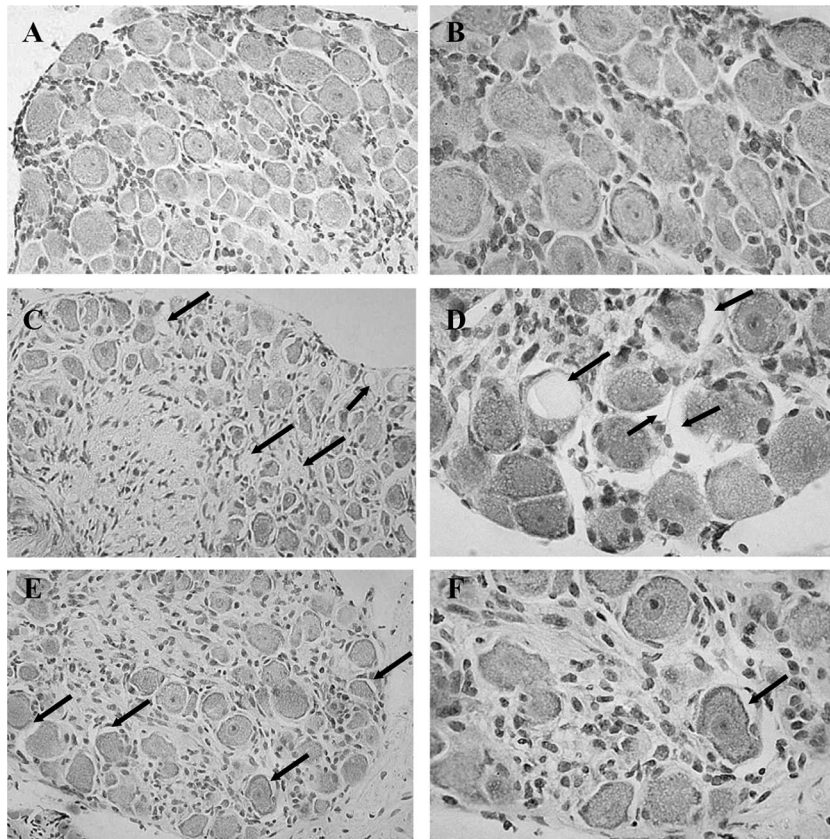


FIG. 5. Histological examination of DRG obtained from mice at 6 days p.i. with  $10^6$  PFU of HSV-1. (A) A ganglion from a wt C57BL/6 mouse contains neurons that are normal morphologically and closely apposed to each other. (B) At a higher magnification, the neuronal bodies are seen to be intact, have ovate nuclei, and surrounded by satellite cells. (C) In contrast, a DRG from a CD1d GKO mouse shows fewer neurons, evidence of neuronal "drop-out" (arrows), and increased intercellular connective tissue. (D) At a higher magnification, neuronal bodies are vacuolated, and some (arrowed) show shrinkage from the supporting satellite cells. (E) A section of a DRG from a  $J\alpha 18$  GKO mouse has an appearance similar to that from CD1d GKO (see panel C). (F) At a higher magnification, neurons are seen to be widely separated and vacuolated in appearance, and there is shrinkage (arrow) from satellite cells. A, C, and E,  $\times 20$  objective; B, D, and F,  $\times 40$  objective.

of  $J\alpha 18$  GKO mice and CD1d GKO mice infected with HSV-1 were similar in our previous study (15), this similarity could reflect unintended selection of mice that survived beyond day 5 p.i. infection (i.e., those with sublethal loads of virus). In the present study, mortality was observed to be greater in CD1d GKO mice than in  $J\alpha 18$  GKO mice. We postulated, therefore, that the lesser mortality in the  $J\alpha 18$  GKO mice was related to the presence in these mice of NKT cells with diverse TCRs. This subset of NKT cells has been shown to contribute to protective immunity against several other viruses (4, 12, 13). We postulated also that the effects of these cells might be more prominent at doses of virus that produced lower mortality.

Mortality was reduced by inoculating CD1d GKO,  $J\alpha 18$  GKO, and wt mice with either  $5 \times 10^5$  PFU or  $1 \times 10^5$  PFU of HSV-1 (SC16). These doses are 0.5 and 1.0 logs lower, respectively, than the standard dose used above and that used by Grubor-Bauk et al. (15). After infection with  $5 \times 10^5$  PFU of virus (Fig. 6A), the survival of  $J\alpha 18$  GKO mice (90%, 18/20) was comparable to that of wt mice (95%, 19/20). Although the survival of CD1d GKO mice was higher at this dose of virus (50%, 10/20) than in mice receiving  $10^6$  PFU (33%, 15/46) (Fig. 1), the mortality was much higher than in the  $J\alpha 18$  GKO mice. The proportion of mice with zosteriform lesions (Fig.

6B) was much lower in  $J\alpha 18$  GKO mice at 7 days p.i. (43%) than in CD1d GKO mice (77%) and similar to that in wt mice (47%). Furthermore, the zosteriform lesions in the  $J\alpha 18$  GKO mice were less severe than those in the CD1d GKO mice and comparable in size to those in the wt mice (Fig. 6C and 6D). The difference between the  $J\alpha 18$  GKO and CD1d GKO mice was most pronounced at day 9 p.i., when the mean lesion width in CD1d GKO mice was  $\sim 5$  mm, whereas lesions in most of the  $J\alpha 18$  GKO and wt mice had healed and those remaining had a mean width of 2 mm (Fig. 6E). Nevertheless, by day 12 p.i., skin lesions in all of the surviving animals in each group had healed (data not shown). At day 7 and day 9 p.i. lesion sizes were not significantly different between wt and  $J\alpha 18$  GKO but were significantly different than those in CD1d GKO mice ( $P < 0.01$ ).

In mice infected with the lowest dose of virus ( $10^5$  PFU), all wt and  $J\alpha 18$  GKO mice survived, but there was still 20% (4/20) mortality in the CD1d GKO mice (Fig. 7A). None of the wt mice displayed initial signs of infection in the skin (such as swelling and edema at the site of scarification) or developed zosteriform lesions (Fig. 7B and C). In contrast, initial signs of infection were present in CD1d GKO mice and by day 7 p.i., 23% (4/18) had developed severe zosteriform lesions (Fig. 7B

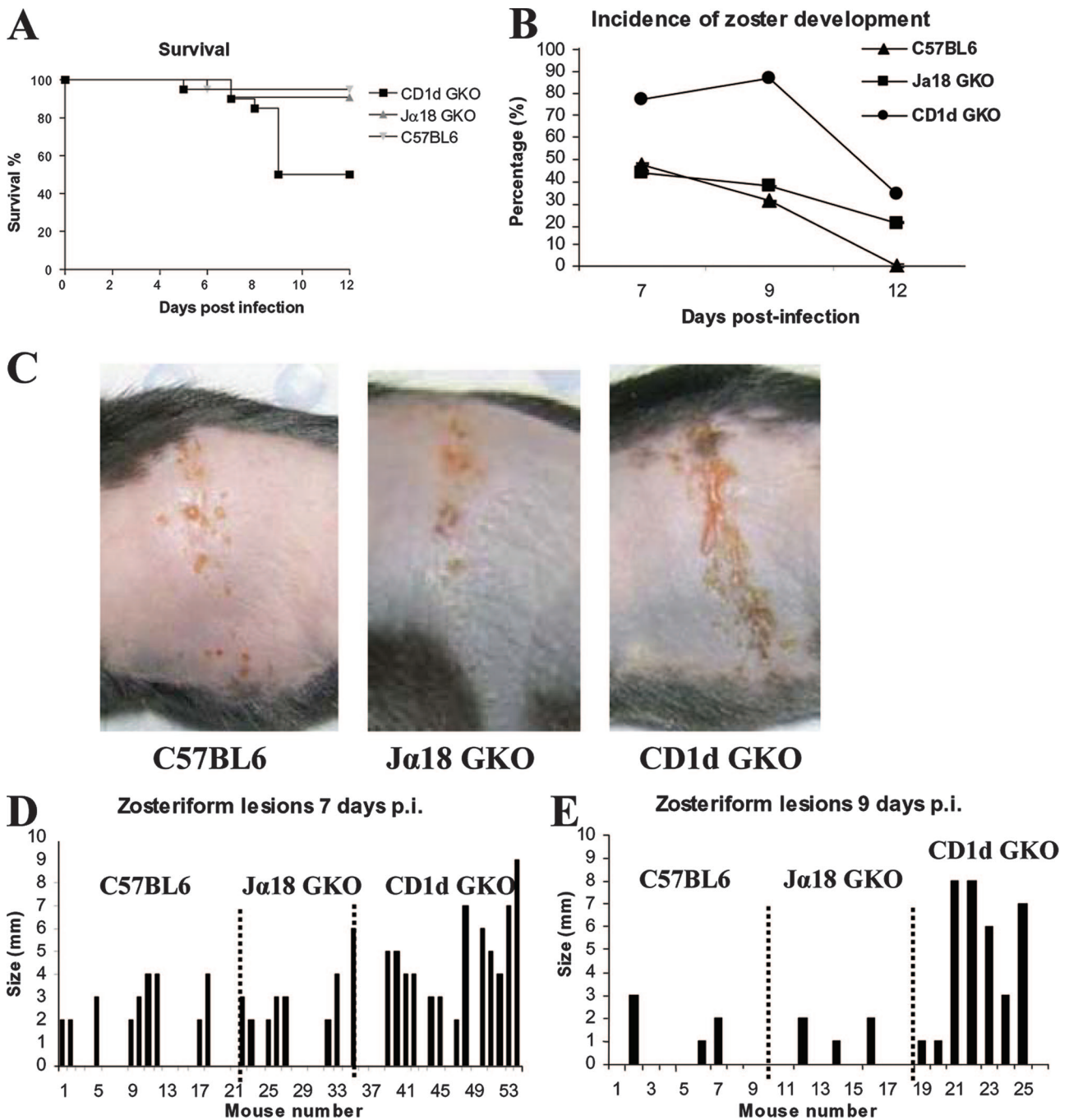


FIG. 6. Survival and sizes of zosteriform lesions in NKT-cell-deficient mice infected with  $5 \times 10^5$  PFU of HSV-1 (SC16). J $\alpha$ 18 GKO, CD1d GKO, and C57BL/6 mice were infected and monitored daily ( $n = 20$ ). (A) Survival was similar in J $\alpha$ 18 GKO and C57BL/6 mice but significantly lower in CD1d GKO ( $P = 0.001$ ) mice as analyzed by the Kaplan-Meier method. (B) The incidence of zosteriform lesions was lower in J $\alpha$ 18 GKO and C57BL/6 mice than in CD1d GKO mice. (C) At 7 days p.i., the lesions were significantly more severe in CD1d GKO mice than in J $\alpha$ 18 GKO mice and C57BL/6 mice (one-way ANOVA with Tukey's post hoc test,  $P < 0.01$ ). (D) The size of lesions (width in millimeters) was significantly smaller in J $\alpha$ 18 GKO and C57BL/6 mice than in CD1d GKO mice at 7 days p.i. (one-way ANOVA with Tukey's post hoc test,  $P < 0.01$ ). (E) In the remaining mice most of the lesions in J $\alpha$ 18 GKO and C57BL/6 mice had healed by day 9 p.i., but large lesions persisted in some CD1d GKO mice.

to D). In J $\alpha$ 18 GKO mice, there were small areas of vesicles around the site of inoculation but only 10% (2/20) developed zosteriform lesions by day 7 p.i. (Fig. 7C and D). Only CD1d GKO mice had zosteriform lesions at day 9 p.i. (Fig. 7E). At

days 7 and 9 p.i. the lesion sizes were not significantly different between wt and J $\alpha$ 18 GKO mice but were significantly different than those in CD1d GKO mice ( $P < 0.05$ ). In summary, at lower doses of virus, resistance of J $\alpha$ 18 GKO mice is compa-

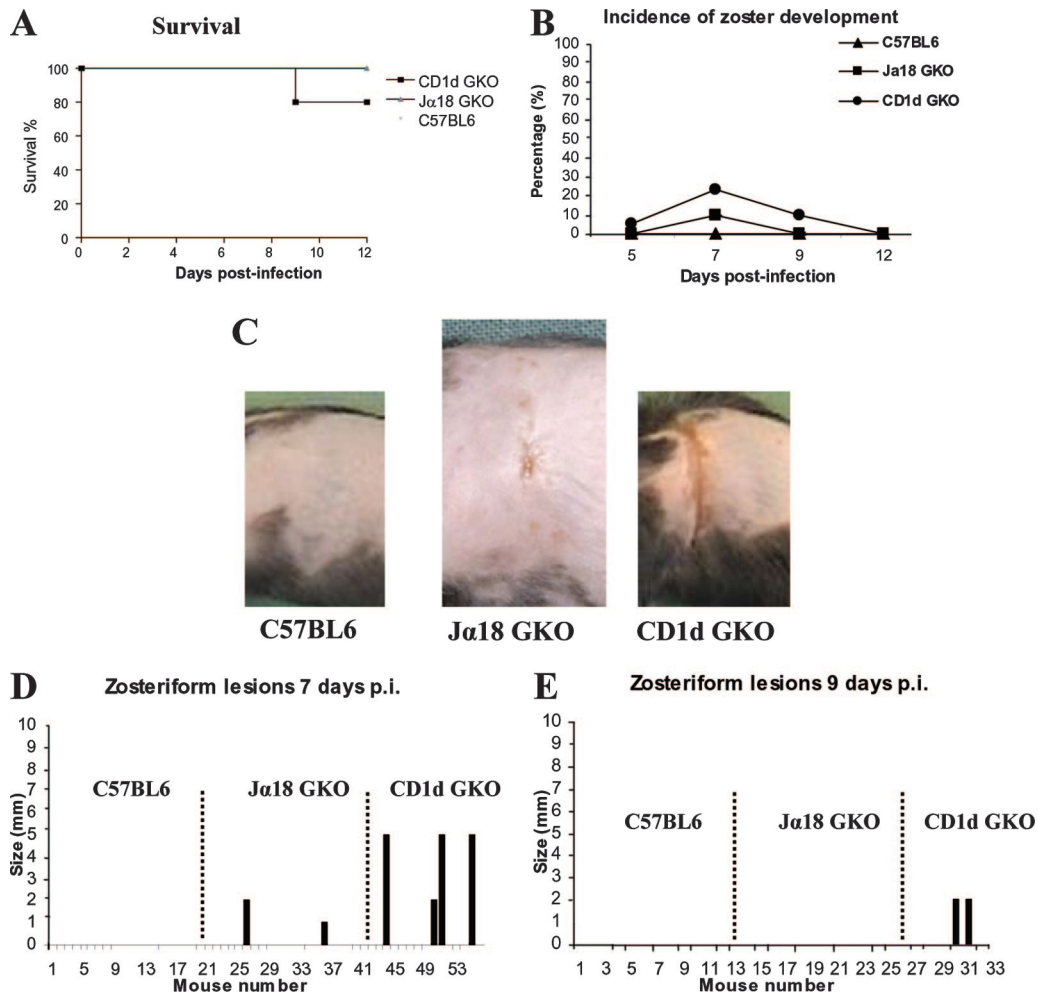


FIG. 7. Survival and sizes of zosteriform lesions in NKT-cell-deficient mice infected with  $10^5$  PFU of HSV-1. Jα18 GKO, CD1d GKO, and C57BL/6 mice (~20 per group) were infected and monitored daily. (A) All Jα18 GKO and C57BL/6 mice survived, but there was a mortality of 20% in the CD1d GKO mice as analyzed by the Kaplan-Meier method ( $P = 0.01$ ). (B) Zosteriform lesions were not observed in C57BL/6 mice and in only 5% of Jα18 GKO. However, they were present in 30% of the CD1d GKO mice. (C) At day 7, a Jα18 GKO mouse has scattered vesicles, but the zosteriform lesion in a CD1d GKO mouse is moderate to severe. (D) The lesions present in two Jα18 GKO mice were small at 7 days p.i. (width in millimeters), but those in four affected CD1d GKO mice were of moderate to severe extent. (E) Lesions were still present in two of the CD1d GKO mice by day 9 p.i. but had healed in the other two mice. The lesions of CD1d GKO mice were significantly more severe at days 7 and 9 than those of Jα18 GKO and C57BL/6 mice (one-way ANOVA with Tukey's post hoc test; day 7,  $P < 0.05$ ; day 9,  $P < 0.01$ ).

rable to wt mice. However, continuing mortality and morbidity at even the lowest dose in the CD1d GKO mice indicates the importance of type II NKT cells in resistance to virulent neuropathic HSV-1. This notion was further supported by examining the virus load in skin and ganglia of all three types of mice using the two lower doses, during the acute stage of HSV-1 infection (see Fig. S1 in the supplemental material).

**Comparison of latent infection in CD1d GKO and Jα18 GKO mice.** During latent infections in sensory neurons of DRG, there is an abundance of LATs. The presence of LATs provides a valuable "footprint" with which to track the anatomical spread of the virus, as well as the frequency of latency in sensory neurons. CD1d GKO and Jα18 GKO mice were inoculated with  $10^6$  PFU of virus on the left flank and both ipsilateral and contralateral DRG (T8 to T13) were collected from groups of five survivors 30 days later. LATs were detected by in situ hybridization in histological sections cut from

blocks containing the separately pooled ipsilateral and contralateral DRG from each mouse. Counts were made of the number of DRG profiles that contained LATs and of the total number of DRG profiles on each slide, allowing calculation of the percentage of LAT-positive ganglia.

Approximately 70% of the profiles of ipsilateral DRG from CD1d GKO and Jα18 GKO mice contained LAT RNA-positive neurons compared to only 20% in wt mice (Fig. 8A), indicating that a higher proportion of the DRG were infected and subject to latency in the NKT-cell-deficient mice. These findings were consistent with the higher incidence of zosteriform lesions observed in Jα18 GKO mice (above) and CD1d GKO mice (15). It was surprising, however, that ~70% of the profiles of DRG from the side contralateral to infection in CD1d and Jα18 GKO mice contained LAT RNA-positive neurons (Fig. 8B). In contrast, LATs were detected in only 5% of the contralateral DRG from the wt mice. It appears, therefore,

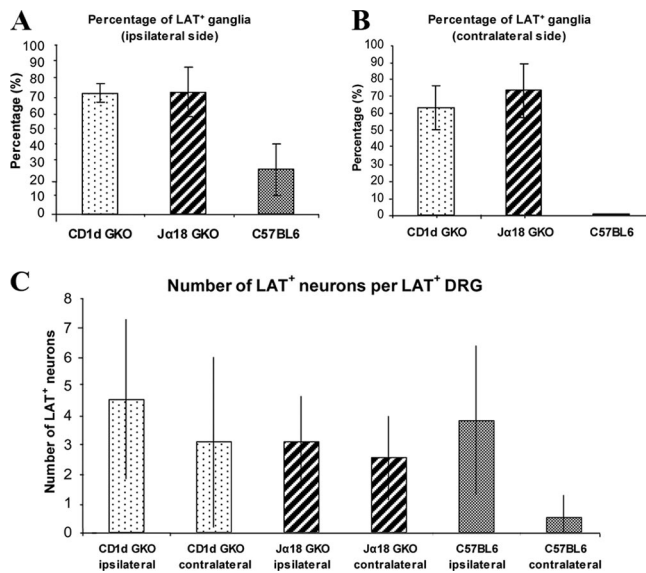


FIG. 8. Expression of LATs in DRG from CD1d GKO, J $\alpha$ 18 GKO, and C57BL mice infected with HSV-1 (SC16). At 28 days p.i. ( $10^6$  PFU,  $n = \sim 30$  per group), DRG (T8 to T13) were removed from the sides ipsilateral and contralateral to the site of infection in each mouse and embedded together in a block. The percentage of LAT<sup>+</sup> DRG was calculated for each block containing ipsilateral (A) or contralateral (B) ganglia. (C) The number of LAT<sup>+</sup> neurons per LAT<sup>+</sup> ganglion was calculated after examination of  $\sim 20$  sections per block. Each point represents the geometric mean ( $\pm$ range) from groups of  $\sim 20$  slides per block.

that the virus can traverse the spinal cord and established latency in a high proportion of the contralateral DRG in both of the GKO strains. This finding is consistent with a higher incidence of hind limb paralysis observed in these strains after inoculation with the standard dose of virus (not shown).

To characterize latency at the single cell level, the numbers of LAT-expressing neurons were estimated per LAT-positive ganglionic profile. The numbers of LAT RNA-positive neurons per ipsilateral DRG profile were not significantly different between CD1d GKO and J $\alpha$ 18 GKO mice and, interestingly, there was no significant difference between the numbers in ipsilateral DRG from wt mice versus those from GKO mice (Fig. 8C). However, on the side contralateral to infection, very few ( $\leq 1$ ) LAT RNA-positive neurons were observed in any of the DRG from wt mice. In contrast, LAT RNA-positive neurons were almost as frequent in DRG from the contralateral and ipsilateral sides in the NKT-cell-deficient mice, and there was no significant difference between the CD1d GKO and J $\alpha$ 18 GKO strains. Taken together, the results indicate that spread of the virus across the spinal cord is limited in wt mice compared to NKT-cell-deficient mice and that NKT cells expressing the invariant TCR are sufficient to limit this spread.

## DISCUSSION

The clinical outcome of an infection with HSV-1 can be considered as a race between progression of the infection and the deployment of host defenses (14). The race will be lost if the virus load exceeds the capacity of a fully competent adaptive immune system to prevent systemic disease and invasion of

the CNS. In the zosteriform model, local replication and spread of virus in the skin occurs during the period 14 to 48 h after infection (1). This early amplification ensures access of the virus to the DRG via sensory nerve endings and thus has a major influence on the subsequent clinical manifestations of the infection. It can be expected that early defense mechanisms will be critical in preventing virus load from reaching the tipping point beyond which infection leads to serious disease. For this reason, NKT cells are of interest because they are believed to promote rapid innate and adaptive immune responses (for reviews, see references 41 and 42). In the discussion that follows, HSV-1 infection is considered to have an afferent phase, during which the virus proliferates first in the skin and later in the DRG. During this period, comparisons of virus loads in wt and null mice provide a clear picture of the importance of NKT cells in controlling virus replication at these sites. The afferent phase is followed by anterograde spread to dermatomes supplied by the infected DRG, establishment of latency and, in some cases, spread to the CNS. These outcomes provide a more global insight into the importance of NKT cells in defense against HSV-1.

Critical determinants of outcome in HSV-1 infections will be the inoculation dose (which is probably low in natural infections) and the virulence of the virus. Reports from a number of laboratories indicate that as a group, low-passage clinical isolates such as SC16 behave differently than laboratory strains such as KOS (6, 11, 14). Comparison of the KOS strain with several highly neuroinvasive strains of HSV-1 in a zosteriform model showed that potential to invade the CNS correlates with the severity of zosteriform lesions, the percentage of mice exhibiting zosteriform lesions, and mortality (14). Neuroinvasive potential followed the trend: low-passage nervous system isolates  $\geq$  low-passage non-nervous system isolates  $\gg$  highly passaged laboratory strains (11, 14). This is relevant because a recent study in CD1d GKO mice concluded that NKT cells (type I and type II) are not critical for protection against the KOS strain of HSV-1 (8), contrasting with our own observations that disease was more severe in CD1d GKO mice infected with the neuropathic strain SC16 than in wt controls (15). Compared to the KOS strain (6, 10, 11, 14, 39), a neurovirulent clinical isolate such as SC16 can be expected to exercise the full range of host defenses, and we show here that important differences in the susceptibility of CD1d GKO mice, J $\alpha$ 18 GKO mice, and wt mice to SC16 are dependent on inoculation dose.

Our previous study showed that after inoculation of  $10^6$  PFU, the virus load in skin at day 3 was similar in CD1d GKO mice and wt controls, indicating that proliferation during the early afferent phase of infection was similar with or without NKT cells. However, virus load was higher in DRG, more ganglia were infected, virus persisted longer, and there were larger amounts of virus antigen in the CD1d GKO mice (15). This indicated that NKT cells play a significant role in controlling HSV-1 spread and replication in DRG. Larger zosteriform lesions in CD1d GKO mice and higher virus loads in the skin later in the infection were consistent with this conclusion. However, virus loads were similar in DRG from CD1d GKO mice (absence of all NKT cells) and J $\alpha$ 18 GKO mice (absence of type I NKT cells only), suggesting that type II NKT cells did



not provide additional protection during the afferent phase of infection.

We have extended the comparison of J $\alpha$ 18 GKO mice and wt mice, using the standard inoculation dose of  $10^6$  PFU. In the afferent phase of the infection, virus loads in the skin were higher in J $\alpha$ 18 GKO mice than in wt controls at 3 days p.i. Thus, in this experiment, virus replication was greater in the absence of type I NKT cells, whereas we found previously (15) that virus loads were similar in wt and CD1d GKO mice, which lack both type I and type II NKT cells. The reason for this apparent discrepancy has not been investigated further. Virus loads in DRG from J $\alpha$ 18 GKO mice were higher than in wt mice, as found in our previous study (15), and large numbers of neurons continued to express viral antigen after it had been cleared from DRG in wt mice. It is clear, therefore, that the lack of type I NKT cells allowed greater replication of virus during the afferent phase of infection. Furthermore, there was considerable death of sensory neurons in the DRG of J $\alpha$ 18 GKO mice and CD1d GKO mice, suggesting that the type I subset in particular is important in limiting neuronal death.

The late outcomes of infection in these mice were of particular interest. Zosteriform lesions developed in a higher proportion of the J $\alpha$ 18 GKO mice, they were apparent earlier and were more extensive than in wt mice. These findings indicate that type I NKT cells provide overall protection against spread of the virus via the peripheral nervous system. Mortality or severe morbidity requiring euthanasia was higher in J $\alpha$ 18 GKO mice than in wt mice, but the incidence of life-threatening disease was most striking in CD1d GKO mice. Some NKT-cell-deficient mice exhibited hind limb paralysis, suggesting transverse myelitis caused by virus invasion of the spinal cord. It was of significance, therefore, that latency was detected in contralateral DRG from many of the surviving CD1d and J $\alpha$ 18 GKO mice, confirming that transmission via the spinal cord had indeed occurred in these mice. It appears, therefore, that while type I NKT cells offer some protection against these severe outcomes, type II NKT cells (or a combination of both subsets) are necessary to provide resistance equivalent to that of wt mice.

These findings raised the possibility that the relatively high mortality and morbidity in null mice infected with  $10^6$  PFU had masked differences in resistance between the CD1d and J $\alpha$ 18 GKO strains that might have been apparent at lower doses of virus. This proved to be the case, because the survival of J $\alpha$ 18 GKO mice and wt mice was equal at inoculation doses of  $5 \times 10^5$  and  $1 \times 10^5$  PFU. In contrast, mortality in CD1d GKO mice was essentially the same at  $5 \times 10^5$  PFU as at  $1 \times 10^6$  PFU. It was only at a dose of  $10^5$  PFU that survival increased in CD1d GKO, reaching  $\sim 80\%$  of that in J $\alpha$ 18 GKO mice and wt mice. The dose of  $10^5$  PFU appears to represent a threshold at which mechanisms that are independent of either type I or type II NKT cells can provide some assistance in preventing early death in CD1d GKO mice. Conversely, only at the highest dose ( $10^6$  PFU) was there a discernible difference in mortality between J $\alpha$ 18 GKO mice and wt mice that could be attributed to the effects of type I NKT cells. The differences between CD1d and J $\alpha$ 18 GKO mice were also evident when the incidence and severity of zosteriform lesions were compared. J $\alpha$ 18 GKO mice and wt mice were indistinguishable at all doses of virus, while some CD1d GKO mice exhibited

extensive zosteriform lesions even at the lowest dose. Virus loads in skin and DRG were consistent with the size and incidence of the zosteriform lesions. In particular, at the lowest dose, infectious virus was detected in the skin of some CD1d GKO mice but in neither J $\alpha$ 18 GKO mice nor wt mice. These findings show that at doses of neurovirulent HSV-1 that are subclinical in J $\alpha$ 18 GKO mice and normal mice, type II NKT cells are critical in preventing the early establishment of infection and severe or fatal outcomes. This conclusion is supported by the observation (not shown) that the proportions of NK1.1<sup>+</sup>  $\alpha\beta$ TCR<sup>+</sup> cells in the spleens of J $\alpha$ 18 GKO mice are essentially normal ( $\sim 0.75\%$ , compared to  $\sim 2\%$  in wt mice). However, the difference in survival of wt mice relative to J $\alpha$ 18 GKO mice at the highest dose of virus is due to the effects of type I NKT cells, which we have shown to control invasion of the central nervous system.

Finally, because NKT cells contribute to limiting the spread of HSV-1, they also reduce the level of latency in DRG. No difference was observed between levels of latency in CD1d and J $\alpha$ 18 GKO mice, either in terms of the proportion of LAT-positive DRG or the proportion of LAT-positive neurons. It appears, therefore, that the type I subset of NKT cells is as effective in determining level of latency as the activities of the combined subsets. This conclusion is consistent with the effectiveness of type I NKT cells (see above) in helping to limit virus replication and spread during the afferent phase of infection. It was noteworthy, therefore, that although the proportion of LAT-positive DRG was higher in both strains of GKO mice than in wt mice, the proportion of LAT-positive neurons was similar in all strains. Histological examination of DRG from infected mice showed that neuronal death was higher in the NKT-cell-deficient mice. The simplest interpretation of equivalent proportions of LAT-positive neurons in DRG from the NKT-cell-deficient strains and wt mice is that many infected neurons die in CD1d and J $\alpha$ 18 GKO mice and do not enter the latently infected pool. Thus, earlier control of virus in mice with intact NKT cells limits the loss of sensory neurons but at the price of greater latency and, therefore, a greater burden of cutaneous herpetic lesions in the future.

We have not examined the mechanism by which NKT cells provide protection against infection with HSV-1. However, we have found that the defect in handling of HSV-1 by J $\alpha$ 18 GKO mice can be complemented by adoptive transfer of lymphocytes from wt mice (unpublished data). NKT cells are not essential for the resolution of infection, because some CD1d GKO mice can clear the virus and recover, provided they survive the acute phase of the disease. Our studies show that survival depends critically on the initial dose of virus and, we argue, the virulence of the HSV-1 strain. At sufficiently high doses, a weakly virulent strain such as KOS could overwhelm the protection provided by NKT, and we believe that this could account for the difference in susceptibility to infection of CD1d GKO mice observed in our studies using the neurovirulent SC16 strain and those of Cornish et al. (8) using the less-virulent KOS strain.

In terms of mechanism, recent studies have demonstrated that IL-15, and its action on NK cells and NKT cells, is critical for protection against intravaginal HSV-2 infections (3). IL-15 produced by infected epithelial cells and/or local macrophages is thought to induce production of IFN- $\gamma$  by NK cells and NKT

cells, which in turn has antiviral effects. Nevertheless, systemic control and elimination of infectious virus requires the action of virus-specific CD8<sup>+</sup> T cells (32, 43). Early adoptive transfer of activated virus-specific CD8<sup>+</sup> T cells can reduce or abrogate the course of the zosteriform infection, showing that cytotoxic T cells can limit spread of virus if they are present at the right time and in sufficient numbers (43). The greater severity of infection in NKT-cell-deficient mice may, therefore, be due to slower activation and recruitment of CD8<sup>+</sup> T cells. It is of interest, therefore, that activation of V $\alpha$ 14<sup>+</sup> NKT cells with the CD1d ligand  $\alpha$ -GalCer facilitates the induction of antigen-specific CD8<sup>+</sup> T cells (29). Furthermore, lack of early IFN- $\gamma$  production by V $\alpha$ 14<sup>+</sup> NKT cells, leading to reduced activation, expansion, and/or recruitment of CD8<sup>+</sup> T cells, has been associated with enhanced tissue damage during infections with respiratory syncytial virus (18).

A clear conclusion from our studies is that NKT cells provide an adjunct to the conventional innate and adaptive immune defenses against HSV-1. At doses of neurovirulent virus that may approximate natural infection, these cells appear to have a critical role in determining whether the virus is controlled rapidly or whether there is rapid amplification and escalation toward a lethal outcome. Our results show that both subsets of CD1d-dependent NKT cells participate in enhancing resistance to the virus. While the effects of the two subsets may simply summate, there are indications that the protective activities are delegated to particular sites or stages in the infection. However, it is difficult to assign site-specific functions in this highly interconnected model, and further investigation will require staged adoptive transfers of the purified subsets. It is a fascinating possibility that the subsets might respond to the virus infection via different cues at different locations or stages. For instance, the type II subset might recognize and respond to a diverse range of potential CD1d ligands, while the response of the invariant type I subset is probably restricted to recognition of endogenous molecules, such as isoglobotrihexosylceramide, that are produced by stressed cells (44). A role for NKT cells in determining the outcome of HSV-1 infection at the earliest stages would be consistent with their role in other experimental systems. Early activation of type I NKT cells by  $\alpha$ -GalCer has been shown to increase the production of antigen-specific cytotoxic T cells dramatically (16), possibly by providing early maturation signals to local dendritic cells (16, 36). Furthermore, activation of type I NKT cells by endogenous glycolipid appears to play a vital role in the resistance of mice to certain gram-negative bacteria (25). Incorporation of NKT cell stimulants in new antiviral vaccines could not only increase their protective efficacy but also, by reducing the lag time of response, enhance their usefulness in circumstances that demand immediate protection against infection.

#### ACKNOWLEDGMENTS

This study was supported by a grant for New and Innovative Research Directions from the Faculty of Health Sciences, University of Adelaide. B.G.-B. was the recipient of a Royal Adelaide Hospital Dawes Scholarship.

We thank Masaru Taniguchi for agreeing to our use of J $\alpha$ 18 GKO mice. We are grateful to Gorjana Radisic for assistance with plaque assays and to Irmeli Penttila, and Katie Tooley for assistance with statistical analyses.

#### REFERENCES

- Allan, R. S., C. M. Smith, G. T. Belz, A. L. van Lint, L. M. Wakim, W. R. Heath, and F. R. Carbone. 2003. Epidermal viral immunity induced by CD8 $\alpha$ <sup>+</sup> dendritic cells but not by Langerhans cells. *Science* **301**:1925–1928.
- Arthur, J., S. Efsthathiou, and A. Simmons. 1993. Intranuclear foci containing low abundance herpes simplex virus latency-associated transcripts visualized by non-isotopic in situ hybridization. *J. Gen. Virol.* **74**(Pt. 7):1363–1370.
- Ashkar, A. A., and K. L. Rosenthal. 2003. Interleukin-15 and natural killer and NKT cells play a critical role in innate protection against genital herpes simplex virus type 2 infection. *J. Virol.* **77**:10168–10171.
- Baron, J., L. Gardiner, S. Nishimura, K. Shinkai, R. Locksley, and D. Ganem. 2002. Activation of a nonclassical NKT cell subset in a transgenic mouse model of hepatitis B virus infection. *Immunity* **16**:583–594.
- Benlagha, K., T. Kyin, A. Beavis, L. Teyton, and A. Bendelac. 2002. A thymic precursor to the NK T-cell lineage. *Science* **296**:553–555.
- Bower, J. R., H. Mao, C. Durishin, E. Rozenbom, M. Detwiler, D. Rempinski, T. L. Karban, and K. S. Rosenthal. 1999. Intrastrain variants of herpes simplex virus type 1 isolated from a neonate with fatal disseminated infection differ in the ICP34.5 gene, glycoprotein processing, and neuroinvasiveness. *J. Virol.* **73**:3843–3853.
- Carnaud, C., D. Lee, O. Donnars, S. H. Park, A. Beavis, Y. Koezuka, and A. Bendelac. 1999. Cutting edge: cross-talk between cells of the innate immune system: NK T cells rapidly activate NK cells. *J. Immunol.* **163**:4647–4650.
- Cornish, A. L., R. Keating, K. Kyprissoudis, M. J. Smyth, F. R. Carbone, and D. I. Godfrey. 2006. NKT cells are not critical for HSV-1 disease resolution. *Immunol. Cell Biol.* **84**:13–19.
- Cui, J., T. Shin, T. Kawano, H. Sato, E. Kondo, I. Toura, Y. Kaneko, H. Koseki, M. Kanno, and M. Taniguchi. 1997. Requirement for V $\alpha$ 14 NKT cells in IL-12-mediated rejection of tumors. *Science* **278**:1623–1626.
- Dick, J. W., and K. S. Rosenthal. 1995. A block in glycoprotein processing correlates with small plaque morphology and virion targeting to cell-cell junctions for an oral and an anal strain of herpes simplex virus type-1. *Arch. Virol.* **140**:2163–2181.
- Dix, R. D., R. R. McKendall, and J. R. Baringer. 1983. Comparative neurovirulence of herpes simplex virus type 1 strains after peripheral or intracerebral inoculation of BALB/c mice. *Infect. Immun.* **40**:103–112.
- Durante-Mangoni, E., R. Wang, A. Shaulov, Q. He, I. Nasser, N. Afzal, M. J. Koziel, and M. A. Exley. 2004. Hepatic CD1d expression in hepatitis C virus infection and recognition by resident proinflammatory CD1d-reactive T cells. *J. Immunol.* **173**:2159–2166.
- Exley, M. A., N. J. Bigley, O. Cheng, S. M. Tahir, S. T. Smiley, Q. L. Carter, H. F. Stills, M. J. Grusby, Y. Koezuka, M. Taniguchi, and S. P. Balk. 2001. CD1d-reactive T-cell activation leads to amelioration of disease caused by diabetogenic encephalomyocarditis virus. *J. Leukoc. Biol.* **69**:713–718.
- Goel, N., H. Mao, Q. Rong, J. J. Docherty, D. Zimmerman, and K. S. Rosenthal. 2002. The ability of an HSV strain to initiate zosteriform spread correlates with its neuroinvasive disease potential. *Arch. Virol.* **147**:763–773.
- Grubor-Bauk, B., A. Simmons, G. Mayrhofer, and P. Speck. 2003. Impaired clearance of herpes simplex virus type 1 from mice lacking CD1d or NKT cells expressing the semivariant V $\alpha$ 14-J $\alpha$ 281 TCR. *J. Immunol.* **170**:1430.
- Hermans, I. F., J. D. Silk, U. Gileadi, M. Salio, B. Mathew, G. Ritter, R. Schmidt, A. L. Harris, L. Old, and V. Cerundolo. 2003. NKT cells enhance CD4<sup>+</sup> and CD8<sup>+</sup> T-cell responses to soluble antigen in vivo through direct interaction with dendritic cells. *J. Immunol.* **171**:5140–5147.
- Hill, T. J., H. J. Field, and W. A. Blyth. 1975. Acute and recurrent infection with herpes simplex virus in the mouse: a model for studying latency and recurrent disease. *J. Gen. Virol.* **28**:341–353.
- Johnson, T. R., S. Hong, L. Van Kaer, Y. Koezuka, and B. S. Graham. 2002. NK T cells contribute to expansion of CD8<sup>+</sup> T cells and amplification of antiviral immune responses to respiratory syncytial virus. *J. Virol.* **76**:4294–4303.
- Kawano, T., J. Cui, Y. Koezuka, I. Toura, Y. Kaneko, K. Motoki, H. Ueno, R. Nakagawa, H. Sato, E. Kondo, H. Koseki, and M. Taniguchi. 1997. CD1d-restricted and TCR-mediated activation of V $\alpha$ 14 NKT cells by galactosylceramides. *Science* **278**:1626–1629.
- Khanna, K. M., A. J. Lepisto, V. Decman, and R. L. Hendricks. 2004. Immune control of herpes simplex virus during latency. *Curr. Opin. Immunol.* **16**:463–469.
- Koelle, D. M., and L. Corey. 2003. Recent progress in herpes simplex virus immunobiology and vaccine research. *Clin. Microbiol. Rev.* **16**:96–113.
- Kronenberg, M. 2005. Toward an understanding of NKT cell biology: progress and paradoxes. *Annu. Rev. Immunol.* **23**:877–900.
- Liu, T., K. Khanna, X. Chen, D. Fink, and R. Hendricks. 2000. CD8<sup>+</sup> cells can block herpes simplex virus type 1 (HSV-1) reactivation from latency in sensory neurons. *J. Exp. Med.* **191**:1459–1466.
- Manickan, E., and R. Rouse. 1995. Roles of different T-cell subsets in control of herpes simplex virus infection determined by using T-cell-deficient mouse-models. *J. Virol.* **69**:8178–8179.
- Mattner, J., K. L. Debord, N. Ismail, R. D. Goff, C. Cantu III, D. Zhou, P. Saint-Mezard, V. Wang, Y. Gao, N. Yin, K. Hoebe, O. Schneewind, D. Walker, B. Beutler, L. Teyton, P. B. Savage, and A. Bendelac. 2005. Exoge-

- nous and endogenous glycolipid antigens activate NKT cells during microbial infections. *Nature* **434**:525–529.
26. **McLean, I., and P. Nakane.** 1974. Periodate-lysine-paraformaldehyde fixative: a new fixative for immunoelectron microscopy. *J. Histochem. Cytochem.* **22**:1077–1083.
  27. **Mendiratta, S. K., D. W. Martin, S. Hong, A. Boesteanu, S. Joyce, and L. Van Kaer.** 1997. CD1d1 mutant mice are deficient in natural killer cells that promptly produce IL-4. *Immunity* **6**:469–477.
  28. **Mossman, K. L., and A. A. Ashkar.** 2005. Herpesviruses and the innate immune response. *Viral Immunol.* **18**:267–281.
  29. **Nishimura, T., H. Kitamura, K. Iwakabe, T. Yahata, A. Ohta, M. Sato, K. Takeda, K. Okumura, L. Van Kaer, T. Kawano, M. Taniguchi, M. Nakui, M. Sekimoto, and T. Koda.** 2000. The interface between innate and acquired immunity: glycolipid antigen presentation by CD1d-expressing dendritic cells to NKT cells induces the differentiation of antigen-specific cytotoxic T lymphocytes. *Int. Immunol.* **12**:987–994.
  30. **Russell, W.** 1962. A sensitive and precise assay for herpesvirus. *Nature* **195**:1028–1029.
  31. **Simmons, A., and A. Nash.** 1984. Zosteriform spread of herpes simplex virus as a model of recrudescence and its use to investigate the role of immune cells in prevention of recurrent disease. *J. Virol.* **52**:816–821.
  32. **Simmons, A., and D. C. Tscharke.** 1992. Anti-CD8 impairs clearance of herpes simplex virus from the nervous system: implications for the fate of virally infected neurons. *J. Exp. Med.* **175**:1337–1344.
  33. **Speck, P., and A. Simmons.** 1991. Divergent molecular pathways of productive and latent infection with a virulent strain of herpes simplex virus type 1. *J. Virol.* **65**:4001–4005.
  34. **Speck, P., and A. Simmons.** 1998. Precipitous clearance of herpes simplex virus antigens from the peripheral nervous systems of experimentally infected C57BL/10 mice. *J. Gen. Virol.* **79**:561–564.
  35. **Speck, P., and A. Simmons.** 1992. Synchronous appearance of antigen-positive and latently infected neurons in spinal ganglia of mice infected with a virulent strain of herpes simplex virus. *J. Gen. Virol.* **73**:1281–1285.
  36. **Stober, D., I. Jomantaite, R. Schirmbeck, and J. Reimann.** 2003. NKT cells provide help for dendritic cell-dependent priming of MHC class I-restricted CD8<sup>+</sup> T cells in vivo. *J. Immunol.* **170**:2540–2548.
  37. **Tanigawa, M., J. E. Bigger, M. Y. Kanter, and S. S. Atherton.** 2000. Natural killer cells prevent direct anterior-to-posterior spread of herpes simplex virus type 1 in the eye. *Investig. Ophthalmol. Vis. Sci.* **41**:132–137.
  38. **Taniguchi, M., K. Seino, and T. Nakayama.** 2003. The NKT cell system: bridging innate and acquired immunity. *Nat. Immunol.* **4**:1164–1165.
  39. **Thompson, R. L., M. L. Cook, G. B. Devi-Rao, E. K. Wagner, and J. G. Stevens.** 1986. Functional and molecular analyses of the avirulent wild-type herpes simplex virus type 1 strain KOS. *J. Virol.* **58**:203–211.
  40. **van Dommelen, S., H. Tabarias, M. Smyth, and M. Degli-Esposti.** 2003. Activation of natural killer (NK) T cells during murine cytomegalovirus infection enhances the antiviral response mediated by NK cells. *J. Virol.* **77**:1877.
  41. **Van Kaer, L.** 2007. NKT cells: T lymphocytes with innate effector functions. *Curr. Opin. Immunol.* **19**:354–364.
  42. **Van Kaer, L.** 2004. Regulation of immune responses by CD1d-restricted natural killer T cells. *Immunol. Res.* **30**:139–153.
  43. **van Lint, A., M. Ayers, A. G. Brooks, R. M. Coles, W. R. Heath, and F. R. Carbone.** 2004. Herpes simplex virus-specific CD8<sup>+</sup> T cells can clear established lytic infections from skin and nerves and can partially limit the early spread of virus after cutaneous inoculation. *J. Immunol.* **172**:392–397.
  44. **Zhou, D., J. Mattner, C. Cantu III, N. Schrantz, N. Yin, Y. Gao, Y. Sagiv, K. Hudspeth, Y. P. Wu, T. Yamashita, S. Teneberg, D. Wang, R. L. Proia, S. B. Lavery, P. B. Savage, L. Teyton, and A. Bendelac.** 2004. Lysosomal glycosphingolipid recognition by NKT cells. *Science* **306**:1786–1789.